On robust controllers for active steering systems of articulated heavy vehicles

Article *in* International Journal of Heavy Vehicle Systems · January 2019

DOI: 10.1504/IJHVS.2019.097108

3 authors, including:

Shenjin Zhu
Chalmers University of Technology
12 PUBLICATIONS **68** CITATIONS
SEE PROFILE

Yuping He
Ontario Tech University
81 PUBLICATIONS **674** CITATIONS
SEE PROFILE

On robust controllers for active steering systems of articulated heavy vehicles

Shenjin Zhu and Yuping He*

Department of Automotive, Mechanical
and Manufacturing Engineering,
University of Ontario Institute of Technology,
Oshawa, Ontario, Canada L1H 7K4
Email: Shenjin.Zhu@uoit.ca
Email: yuping.he@uoit.ca
*Corresponding author

Jing Ren

Department of Electrical, Computer
and Software Engineering,
University of Ontario Institute of Technology,
Oshawa, Ontario, Canada L1H 7K4
Email: jing.ren@uoit.ca

Abstract: This paper examines the robustness of different controllers for active steering systems (ASSs) of articulated heavy vehicles (AHVs) in terms of the directional performance. Controllers based on the linear quadratic regulator (LQR) technique were designed for ASSs. The success of the LQR-based controllers is dependent on the accuracy of linear models for AHVs. When designing ASS controllers, linearisation of the AHV models is usually necessary; this results in model inaccuracy and un-modelled dynamics, and the robustness of the LQR-based controllers may be degraded. ASSs for AHVs are assessed in the time-domain, which may lead to an incomplete performance evaluation. This paper assesses the robustness of the ASS controllers designed with the techniques of sliding mode control (SMC), nonlinear sliding mode control (NSMC), and mu-synthesis (MS). The ASS controllers are evaluated using numerical simulation in terms of the trade-off between the manoeuvrability and the lateral stability at high speeds.

Keywords: AHVs: articulated heavy vehicles; ASSs: active steering systems; SMC: sliding mode control; NSMC: nonlinear sliding mode control; MS: mu-synthesis; GA: genetic algorithm; robustness index.

Reference to this paper should be made as follows: Zhu, S., He, Y. and Ren, J. (2019) 'On robust controllers for active steering systems of articulated heavy vehicles', *Int. J. Heavy Vehicle Systems*, Vol. 26, No. 1, pp.1–30.

Biographical notes: Shenjin Zhu received his BS in Mechanical Engineering from Harbin University of Science and Technology in 1994, his MS in Mechanical Engineering from McMaster University in 2011, and his PhD in Mechanical Engineering from University of Ontario Institute of Technology in 2016. His research interests include vehicle dynamics and control, driver modelling, active safety system design and coordination, and autonomous driving of single and multi-unit vehicles.

Yuping He received his PhD in Mechanical Engineering from the University of Waterloo, Canada, in 2002. From 1995 to 1998, he was with Beijing Institute of Technology as an Associate Professor. In 2006, he joined the University of Ontario Institute of Technology (UOIT), where he is now an associate professor in automotive engineering. He published more than 100 journal and conference papers in vehicle system dynamics, design optimisation, and active safety systems. He won a research excellent award at UOIT in 2010. He is an Associate Editor of the *International Journal of Vehicle Performance*. He is a Member of SAE, ASME and CSME.

Jing Ren is currently an Associate Professor in the Faculty of Engineering and Applied Science at University of Ontario Institute of Technology. She obtained her MASc and PhD both from Western University in 2003 and 2005 respectively. She has published more than 50 journal papers and conference papers in the fields of robotics, image processing and automotive technologies. She received the University Faculty Award in 2006 for her pioneer work in medical simulations using haptics.

1 Introduction

Active steering systems (ASSs) have been investigated to improve the manoeuvrability (Rangavajhula and Tsao, 2008; Cheng et al., 2011), enhance the lateral stability (Islam et al., 2012; Kharrazi, 2012; Ding et al., 2013), and achieve a better trade-off between the aforementioned conflicting measures (He and Islam, 2012) of AHVs. The majority of studies in this field are built on the LQR technique (Maciejowski, 1989) without adequate consideration of the ASS controller robustness.

Articulated heavy vehicles (AHVs) with ASSs usually experience uncertainties, e.g., variations of forward speed, road adhesion coefficient, trailer payload (Wang and Tomizuka, 2000), road roughness, wind gusts, and braking/accelerating forces (Yin et al., 2010). The deterministically determined optimal solutions may be meaningless (Palkovics and El-Gindy, 1996; Busch and Bestle, 2014). In reality, an ASS should be designed with an acceptable level of robustness under various operating conditions.

The H_∞ technique has become a powerful tool in handling robustness issue since its invention in the 1980s (Doyle, 1985, 1987). The H_∞ technique treats model uncertainties, un-modelled dynamics, and exogenous disturbances in a systematic manner (Skogestad and Postlethwaite, 2001). It has received recognition and still is a hot topic in single unit vehicle dynamics (Gao et al., 1995; Yin et al., 2010; Doumiati et al., 2013), AHV lateral stability (Palkovics et al., 1994) and automated lane guidance (Wang and Tomizuka, 2000). Compared with single unit vehicle dynamic control, ASS controllers based on the H_∞ technique for AHVs are more difficulty to design and have not received necessary attention and consideration.

In addition to the H_∞ technique, the sliding mode control (SMC) also demonstrates good robustness and invariant properties (Utkin et al., 1999). Since its origination in the former Soviet Union in the 1930s (Kulebakin, 1932; Nikolski, 1934; Utkin et al., 1999) and its spread to the western world with a historic review paper (Utkin, 1977), the SMC

has received wide recognition in multiple engineering fields (Lin et al., 2002; Fernandes and Alcalde, 2007; Habibi and Richards, 1992). The SMC technique has been applied to the design of controllers for various systems of passenger cars (Mao and Lu, 2008) and to AHV dynamic control (Oreh et al., 2014).

The lateral dynamics of AHVs, and rearward amplification (RA) in particular, demonstrates frequency-dependent property (Aurell and Winkler, 1995). The majority of the lateral dynamics studies for AHVs (Palkovics and El-Gindy, 1996; Miege and Cebon, 2005; Cheng and Cebon, 2008; He et al., 2010; Islam et al., 2012; Huang et al., 2012; Ding et al., 2012) focus on the performance measures evaluated mainly in the time-domain. However, as pointed out by Aurell and Winkler (1995), the time-domain performance measures of the RA provide only composite information under a specific manoeuvre; for complete RA information of an AHV in a frequency range of interest, the frequency-domain measures are preferred.

To address this issue, Zhu and He (2015) proposed a novel automated frequency response measurement method (AFRM) for acquiring the RA measures for AHVs. With the AFRM technique, a repetitive frequency measurement using sine waves of various frequencies and amplitudes is assigned to a computer in such a way that signal generation, model simulation, and frequency response measurement can be conducted in real-time and online manners. Most importantly, the AFRM technique makes frequency-domain optimisation of the AHV dynamics achievable.

This paper intends to examine the robustness of different controllers for an ASS, by which the steer angles of the tractor rear axle wheels and the semitrailer axle wheels are manipulated, in terms of the directional performance of the tractor/semitrailer (TST). To this end, a three degrees of freedom (DOF) linear yaw-plane TST model is generated to design the controllers using the SMC and MS techniques; a three DOF nonlinear yaw-plane model is derived to devise the controller based on the NSMC method; the performance measures of these controllers are assessed using the co-simulations in the time- and frequency-domain through integration of the controllers designed in Matlab/Simulink and a nonlinear TST model developed in TruckSim. The performance measure of the TST with the ASS in the frequency-domain is acquired using the AFRM technique, and the controllers are optimised using a genetic algorithm (GA) in such a way that the rearward amplification (RA) remains in the vicinity of 1.0 for the optimal trade-off between the high-speed manoeuvrability and stability in a frequency range of interest. The controllers are also evaluated using simulations in the time-domain at low and high lateral accelerations. In the case of simulations in the time-domain, a robustness index is defined to quantify the robustness in terms of the performance measure of the AHV with different ASS controllers.

The rest of the paper is organised as follows. Section 2 introduces the linear and nonlinear yaw-plane models as well as the nonlinear TruckSim model for the TST. Section 3 describes the ASS controllers designed in Matlab/Simulink software using the SMC, NSMC and MS techniques. The ASS controllers designed in Matlab/Simulink and the nonlinear TST model developed in TruckSim are integrated for co-simulation. Section 4 examines the robustness of the ASS controllers based on the SMC, NSMC, MS and LQR techniques by analysing the simulation results in the time- and frequency-domain. Finally, conclusions are drawn in Section 5.

2 Tractor/semitrailer modelling

Three models, namely, the three DOF linear yaw-plane model, three DOF nonlinear yaw-plane model, and the TruckSim model of a TST, are generated. The TST consists of a tractor with 2 axles and a semitrailer with a 3-axle group. As shown in Figure 1, for the three DOF yaw-plane models, a single wheel is employed to represent the tractor front and rear axle and the semitrailer axle group (Palkovics et al., 1994; Palkovics and El-Gindy, 1996). The motions considered in the yaw-plane models include:

- tractor side-slip angle β_1
- tractor yaw rate $\dot{\psi}_1$
- articulation angle $\Delta\psi$ between the tractor and semitrailer.

A linear tyre model is used for the linear yaw-plane model, while for the nonlinear yaw-plane model, the Magic Formula (Pacejka, 2005) is employed.

The following assumptions are made for the yaw-plane models:

- the forward speed is constant and the longitudinal dynamics is negligible
- the vehicle is running on a horizontal surface and the pitch and bounce motions are neglected;
- the articulation angle is small and the forward speeds of all units are equal
- aerodynamics and the load shifting are negligible
- the tyre side-slip angles are small
- all products of variables are ignored.

Figure 1 Yaw-plane model of the tractor/semitrailer

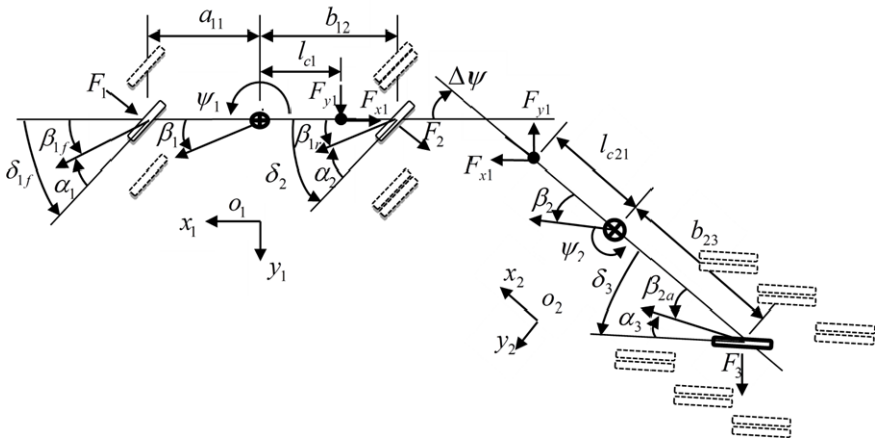

2.1 Three DOF linear yaw-plane model

Using the Newton's law of dynamics, the governing equations of motion for the tractor and semitrailer can be obtained. With the kinematic constraint of the fifth-wheel

connecting the adjacent units, the lateral coupling force can be cancelled. The state space equations of the linear yaw-plane model are expressed as

$$\begin{aligned}\dot{\mathbf{x}} &= \mathbf{A}\mathbf{x} + \mathbf{B}_1\delta_1 + \mathbf{B}\mathbf{u}\\ \mathbf{y} &= \mathbf{C}\mathbf{x} + \mathbf{D}_1\delta_1 + \mathbf{D}\mathbf{u},\end{aligned} \tag{1}$$

where $\mathbf{A}=\mathbf{M}^{-1}\mathbf{P}$, $\mathbf{B}=\mathbf{M}^{-1}\begin{bmatrix}\mathbf{H}_2 & \mathbf{H}_3\end{bmatrix}$, $\mathbf{B}_1=\mathbf{M}^{-1}\mathbf{H}_1$, matrices $\mathbf{C}$, $\mathbf{D}$, $\mathbf{D}_1$, $\mathbf{M}$, $\mathbf{P}$, $\mathbf{H}_1$, $\mathbf{H}_2$ and $\mathbf{H}_3$ are given in Appendix 1, the control variable vector $\mathbf{u}=\begin{bmatrix}\delta_2 & \delta_3\end{bmatrix}^T$, the state variable vector $\mathbf{x}=\begin{bmatrix}\dot{\psi}_1 & \Delta\dot{\psi} & \beta_1 & \Delta\psi\end{bmatrix}^T$ and the output vector $\mathbf{y}=\begin{bmatrix}a_{y1} & a_{y2}\end{bmatrix}^T$. The notation and nominal values of the vehicle system parameters are provided in Table A1 in Appendix 2.

2.2 Three DOF nonlinear yaw-plane model

The three DOF nonlinear yaw-plane model can be obtained by replacing the linear tyre model in equation (1) with the Magic Formula (Pacejka, 2005). The state space equations of the nonlinear yaw-plane model are derived as

$$\begin{aligned}\dot{\mathbf{x}} &= \mathbf{A}_{nl}\mathbf{x} + \mathbf{B}_{nl}F\\ \mathbf{y} &= \mathbf{C}_{nl}\mathbf{x} + \mathbf{D}_{nl}F,\end{aligned} \tag{2}$$

where $\mathbf{A}_{nl}=\mathbf{M}^{-1}\mathbf{P}_{nl}$, $\mathbf{B}_{nl}=\mathbf{M}^{-1}\mathbf{H}_{nl}$, matrices $\mathbf{C}_{nl}$, $\mathbf{D}_{nl}$, $\mathbf{P}_{nl}$, $\mathbf{H}_{nl}$ are given in Appendix 1, and the lateral tyre force component of the vector $F=\begin{bmatrix}F_1 & F_2 & F_3\end{bmatrix}^T$ is calculated as

$$F_i = D_i \sin\left(C_i \arctan\left\{B_i\alpha_i - E_i\left[B_i\alpha_i - \arctan\left(B_i\alpha_i\right)\right]\right\}\right),\ i=1,2,3, \tag{3}$$

where B_i, C_i, D_i, and E_i are the Magic Formula parameters tuned to match the responses of the nonlinear yaw-plane model with those of the TruckSim model.

2.3 TruckSim model

An excellent description of the TruckSim model can be found in a previous work (Islam et al., 2014). The TruckSim package is based on a symbolic multibody program, VehicleSim (VS) Lisp, to generate equations of motion for 3D multibody vehicle systems (MSC, 2014). The TST is defined as '*S_S* + *SSS*', where '*S*' indicates a solid axle, an underscore '_' a separation of axle groups, and a '+' a fifth-wheel connecting the adjacent vehicle units. Thus, as the configuration indicated, the TST consists of a 2 solid-axle tractor having one front axle and one rear axle, and one semitrailer having three solid axles.

In the TruckSim model, the motions considered are as follows. Each of the sprung masses is considered as a rigid body with five DOF, namely, lateral, vertical, pitch, roll and yaw. The forward speed of the tractor is assumed to remain constant under any manoeuvre. Thus, the longitudinal DOF is not included. The fifth wheel is modelled as a ball-joint, about which roll, yaw, and pitch motions are allowed. Each axle is treated as a beam axle that can roll and bounce with respect to the sprung mass to which it is

attached. Each wheel is modelled with a rotatory DOF. Thus, the TST has 26 DOF in total.

2.4 Model validation using time-domain simulation

The yaw-plane and TruckSim models for the TST are first compared using the simulation results in the time-domain achieved under a single cycle sine wave lateral acceleration (SCSLA) test manoeuvre specified in SAE J2179 (SAE, 1993) with the defined trajectory shown in Figure 2. The predefined trajectory is tracked by the tractor at speed of 88 km/h to generate peak lateral acceleration around 0.15 g. The driver model built in TruckSim is employed to 'drive' the TST models. The parameters of the driver model, e.g., preview time and time lag, are tuned in such a way that the lateral acceleration response of the tractor mimics the designated lateral acceleration as close as possible, while the trajectory of tractor CG remains within the ±150 mm tolerance from the defined path. The time histories of the lateral acceleration of the tractor and semitrailer for all the models are shown in Figure 3. Compared with the linear yaw-plane model, the nonlinear yaw-plane model achieves a better agreement with the TruckSim model, especially in terms of the lateral acceleration response of the semitrailer.

Figure 2 Defined trajectory of the CG of the tractor under the SCSLA manoeuvre

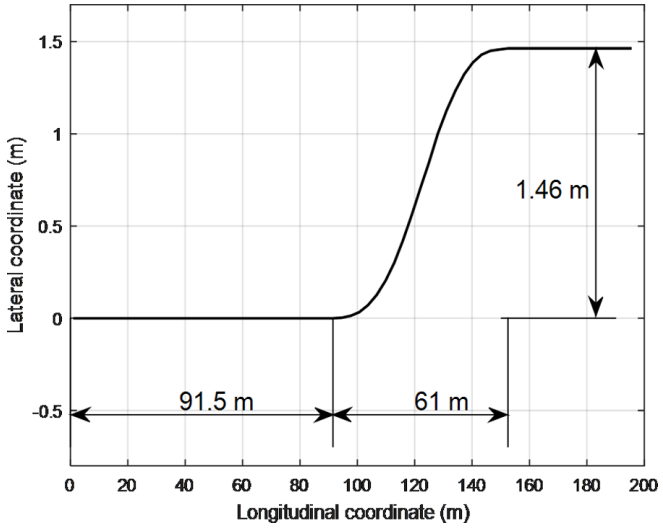

2.5 Model validation using frequency-domain simulation

To validate the yaw-plane models with the TruckSim model using frequency-domain simulation, the magnitude responses are acquired using the AFRM technique in the frequency range of 0 Hz to 1 Hz, motivated by a previous work (Ervin and MacAdam, 1982). The TST models are excited using a multi-cycle sine wave steer input (MCSSI) to minimise transient effect (Zhu et al., 2017).

Figure 4 shows the RA (rearward amplification ratio in lateral acceleration) frequency functions of the TST models, Figure 5 the frequency functions of the gain of the tractor lateral acceleration with respect to the steering wheel angle, and Figure 6 the frequency

functions of the gain of the semitrailer lateral acceleration with respect to the steering wheel angle. The frequency responses disclose interesting insights:

- the three DOF yaw-plane models only capture the main trend of the frequency response of the nonlinear TruckSim model
- the validated time-domain yaw-plane models cannot guarantee a good agreement with the TruckSim model in the frequency range of interest
- the yaw-plane models used to design the ASS controllers are subjected to model inaccuracy and un-modelled dynamics.

The inaccuracy and un-modelled dynamics may be mainly induced by the simplifications, including reduced DOF, neglected nonlinearities, and unconsidered load shifting, which are the main concerns of the capability of the model-based ASS controllers to be designed. The aforementioned insights motivated this research to examine the robustness of different ASS controllers.

Figure 3 Time histories of lateral accelerations of the linear, nonlinear and TruckSim tractor/ semitrailer models under the SCSLA manoeuvre

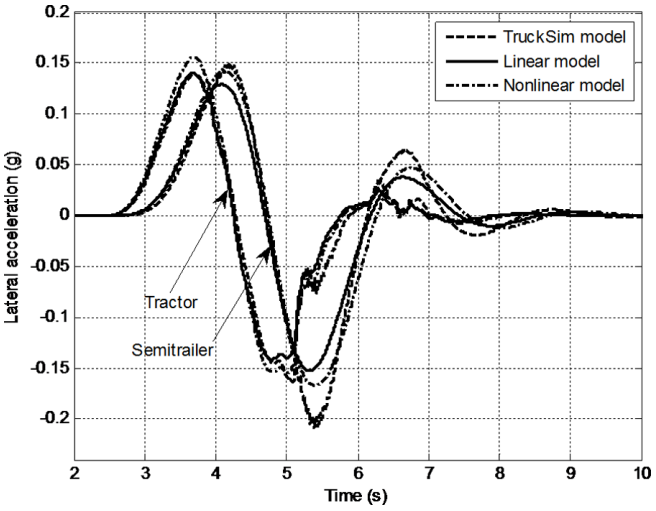

3 Design of ASS controllers

To improve the manoeuvrability and the lateral stability of the TST at high speeds, the following performance measures are minimised:

- the state variables of the yaw-plane models
- the lateral accelerations of the tractor and semitrailer
- the difference between the measured rearward amplification ratio and the desired value of 1.0.

The first two requirements enhance the high-speed stability and the third one improves the trade-off between the manoeuvrability and the lateral stability. Three robust

controllers, namely, the SMC, NSMC and the MS, are designed to achieve robust performance measures of the manoeuvrability and the stability subject to parameter uncertainties and the un-modelled dynamics identified in the previous section. The LQR-based ASS controller similar to the one reported in He and Islam (2012) is also devised as a baseline design for the benchmark study to be conducted in Section 4. The tractor front axle wheel steer angle input is treated as exogenous disturbance; and the active steering angles of the tractor rear axle wheels and semitrailer axle wheels are treated as control variables.

Figure 4 RA frequency functions of the linear and nonlinear yaw-plane models as well as the TruckSim model

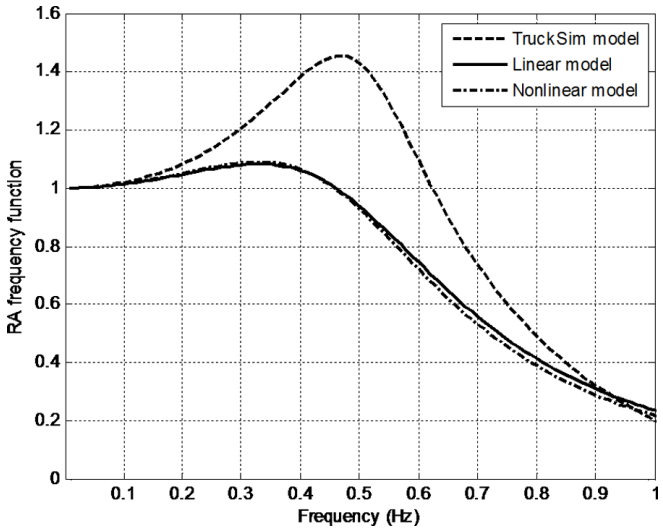

Figure 5 Frequency functions of the gain of the tractor lateral acceleration with respect to the steering wheel angle for the linear and nonlinear yaw-plane models as well as the TruckSim model

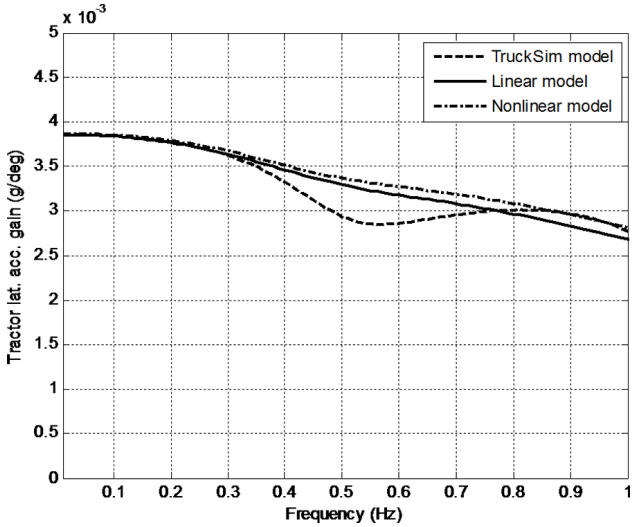

Figure 6 Frequency functions of the gain of the semitrailer lateral acceleration with respect to the steering wheel angle for the linear and nonlinear yaw-plane models as well as the TruckSim model

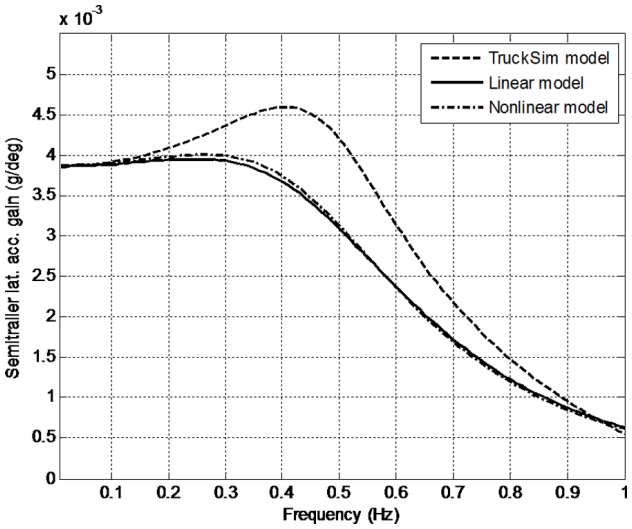

3.1 Controller based on the sliding mode control technique

The first robust controller designed is based on the SMC technique. A typical application of the SMC technique in electromechanical systems is well introduced by Utkin et al. (1999). Reducing the linear yaw-plane model expressed in equation (1) leads to

$$\dot{\mathbf{x}} = \mathbf{A}\mathbf{x} + \mathbf{B}\mathbf{u}, \tag{4}$$

where $\mathbf{u} = \begin{bmatrix} \delta_2 & \delta_3 \end{bmatrix}^T$ denotes the control variable vector, and $\mathbf{x} = \begin{bmatrix} \dot{\psi}_1 & \Delta\dot{\psi} & \beta_1 & \Delta\psi \end{bmatrix}^T$ the state variable vector. The system is time-invariant, and the pair $(\mathbf{A}, \mathbf{B})$ is controllable, and $\operatorname{rank}(\mathbf{B}) = m$ $(m = \dim(\mathbf{u}))$. The state space equation is arranged in such a way that matrix $\mathbf{B}$ can be partitioned as $\mathbf{B} = \begin{bmatrix} \mathbf{B}_1^T & \mathbf{B}_2^T \end{bmatrix}^T$ with $\operatorname{rank}(\mathbf{B}_2) = m$, which requires rearranging the state variable vector as $\mathbf{x} = \begin{bmatrix} \Delta\psi & \dot{\psi}_1 & \Delta\dot{\psi} & \beta_1 \end{bmatrix}^T$. A transformation matrix can be formed as

$$\mathbf{T} = \begin{bmatrix} \mathbf{I}_{n-m} & -\mathbf{B}_1\mathbf{B}_2^{-1} \\ \mathbf{0} & \mathbf{B}_2^{-1} \end{bmatrix}. \tag{5}$$

Transformations are made as $\begin{bmatrix} \mathbf{x}_1 \\ \mathbf{x}_2 \end{bmatrix} = \mathbf{T}\mathbf{x}$, $\begin{bmatrix} \mathbf{A}_{11} & \mathbf{A}_{12} \\ \mathbf{A}_{21} & \mathbf{A}_{22} \end{bmatrix} = \mathbf{T}\mathbf{A}\mathbf{T}^{-1}$, $\mathbf{T}\mathbf{B} = \begin{bmatrix} \mathbf{0} \\ \mathbf{I}_{m\times m} \end{bmatrix}$ and the system expressed in equation (4) is transformed into the regular form (Utkin et al., 1999) as

$$\begin{aligned} \dot{\mathbf{x}}_1 &= \mathbf{A}_{11}\mathbf{x}_1 + \mathbf{A}_{12}\mathbf{x}_2 \\ \dot{\mathbf{x}}_2 &= \mathbf{A}_{21}\mathbf{x}_1 + \mathbf{A}_{22}\mathbf{x}_2 + \mathbf{u}. \end{aligned} \tag{6}$$

The first subsystem expressed in equation (6) can be stabilised by using the pole placement technique (Nise, 2011) to determine a feedback law $\mathbf{x}_2 = -\mathbf{K}_0\mathbf{x}_1$. Thus, a sliding surface can be obtained for the original system as

$$\mathbf{s} = \begin{bmatrix}\mathbf{K}_0 & \mathbf{I}_{m\times m}\end{bmatrix}\mathbf{T}^{-1}\mathbf{x} = \mathbf{G}\mathbf{x}. \tag{7}$$

A control law that continuously minimises the Lyapunov function candidate $V = \frac{1}{2}\mathbf{s}^T\mathbf{s}$ can be obtained (Utkin et al., 1999) as

$$\mathbf{u} = -\left(\alpha|\mathbf{x}| + \delta\right)\text{sign}\left(\mathbf{s}\right), \tag{8}$$

where α and δ are positive design parameters, $|\mathbf{x}| = \sum_{i=1}^{n}|x_i|$ (where $n = \dim(\mathbf{x})$), and $\text{sign}\left(\mathbf{s}\right) = \begin{bmatrix}\text{sign}\left(s_1\right) & \cdots & \text{sign}\left(s_m\right)\end{bmatrix}$. The sign function can be replaced with a saturation function $\text{sat}\left(s_i\right) = \begin{cases} s_i & |s_i/\varepsilon_T|<1 \\ \text{sgn}(s_i) & |s_i/\varepsilon_T|\geq 1\end{cases}, i = 1, 2, \ldots, m$ to eliminate chattering with $\varepsilon_T > 0$ denoting the boundary thickness.

3.2 Controller based on the nonlinear sliding mode control technique

The nonlinear sliding mode control (NSMC) technique presented by Slotine and Li (1991) is frequently used to design a nonlinear model based controller. The NSMC controller designed in this section is based on a yaw-plane model with the lateral tyre forces realised using nonlinear lookup tables. To design the so-called NSMC controller, the state space equation (2) is decomposed into

$$\dot{\mathbf{x}}\left(t\right) = \mathbf{A}_{nl}\mathbf{x}\left(t\right) + \mathbf{B}_{nd}F_1 + \mathbf{B}_{nc}\mathbf{u}_F, \tag{9}$$

where $\mathbf{B}_{nd} = \mathbf{B}_{nl}\left(:,1\right)$ (1st column of $\mathbf{B}_{nl}$) is the disturbance input matrix, $\mathbf{B}_{nc} = \mathbf{B}_{nl}\left(:,2:3\right)$ (2nd and 3rd columns of $\mathbf{B}_{nl}$) the control input matrix, and $\mathbf{u}_F = \begin{bmatrix}F_2 & F_3\end{bmatrix}^T$ the control vector. Removing the disturbance term in equation (9), we have the state space equation for the SMC controller design as

$$\dot{\mathbf{x}}\left(t\right) = \mathbf{A}_{nl}\mathbf{x}\left(t\right) + \mathbf{B}_{nc}\mathbf{u}_F. \tag{10}$$

The SMC controller is designed using the same method presented in Section 3.1 to determine the lateral forces generated by the tractor rear axle wheels and the semitrailer axle wheels as

$$\mathbf{u}_F = -\left(\alpha_F|\mathbf{x}| + \delta_F\right)\text{sign}\left(\mathbf{s}_F\right), \tag{11}$$

where α_F and δ_F are positive design variables and $\mathbf{s}_F$ the sliding surface generated similarly to that expressed in equation (7). Since the lateral tyre forces are calculated by using the Magic Formula in equation (3), i.e., given a side-slip angle, the lateral tyre force can be determined. On the other hand, to realise the lateral tyre force demanded by the SMC controller, a side-slip angle is derived in an inversed Magic Formula, which can be achieved using a look-up table based on the tuned Magic Formula.

The side-slip angles derived from the look-up tables include the 'extra' portion of the side-slip angle of tyres derived from active steering in the kinematical relationships (Zhu and He, 2015) as

$$\begin{aligned}\alpha_2 &= \overbrace{\beta_1 - \left(\frac{b_{12}}{U_1}\right)\dot{\psi}_1}^{\text{state contributed}} + \overbrace{(-\delta_2)}^{\substack{\text{steering}\\ \text{contributed}}},\\ \alpha_3 &= \overbrace{\beta_1 - \Delta\psi - \left(\frac{l_{c21}+b_{23}+l_{c1}}{U_1}\right)\dot{\psi}_1 - \left(\frac{l_{c21}+b_{23}}{U_2}\right)\Delta\dot{\psi}}^{\text{state contributed}} + \overbrace{(-\delta_3)}^{\substack{\text{steering}\\ \text{contributed}}}\end{aligned} \tag{12}$$

The total side-slip angles are contributed from:

- the state variables
- the active steering angles.

Removing the state-contributed portion from the side-slip angles, the required active steering angles by the SMC controller can be determined. Considering the nonlinear property of the look-up tables, we entitle the ASS controller NSMC. The schematic representation of the TruckSim model and the NSMC controller is shown in Figure 7.

Figure 7 Schematic representation of the TruckSim model with the NSMC controller

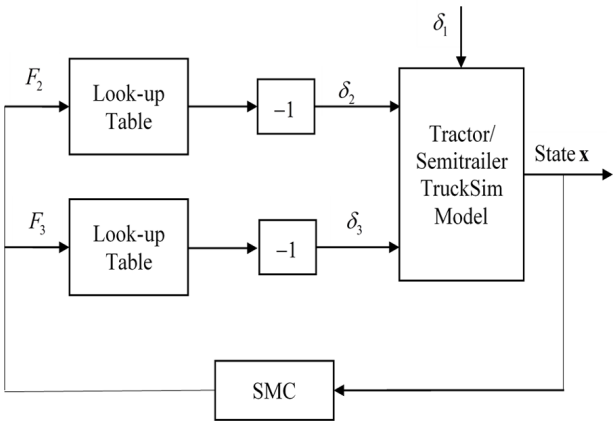

3.3 Controller based on the Mu-Synthesis technique

The controller based on the Mu-Synthesis (MS) technique is one of the commonly used H_∞ controllers, which iteratively solves a mixed sensitivity problem for optimal solution in a frequency range of interest (Skogestad and Postlethwaite, 2001). Uncertain parameters are selected and examined using the frequency-domain parametric sensitivity analysis (Gu et al., 2013) for the parameters determining vehicle kinematics, tyre dynamics and vehicle inertia properties with two criteria:

- the parameters are most sensitive
- the nominal values of the parameters are difficult to obtain.

Model scaling/normalisation makes the model analysis and controller design much simpler (Skogestad and Postlethwaite, 2001). The scaled/normalised variables have their absolute values in the range of (0, 1). The variables, such as the disturbances and the outputs, are normalised with the corresponding expected magnitudes. With the linear yaw-plane model expressed in equation (1) for the MS controller design, the scaled model is given as

$$\begin{cases} \dot{\mathbf{x}} = \mathbf{A}\mathbf{x} + \mathbf{B}\mathbf{U}_{\max}\bar{\mathbf{u}} \\ \bar{\mathbf{y}} = \mathbf{Y}_{\max}^{-1}\mathbf{C}\mathbf{x} + \mathbf{Y}_{\max}^{-1}\mathbf{D}\mathbf{U}_{\max}\bar{\mathbf{u}} \end{cases}, \tag{13}$$

where $\bar{\mathbf{u}} = \begin{bmatrix} \bar{\delta}_1 & \bar{\delta}_2 & \bar{\delta}_3 \end{bmatrix}^T$ denotes the scaled input vector, $\bar{\mathbf{y}} = \begin{bmatrix} \bar{a}_{y1} & \bar{a}_{y2} \end{bmatrix}^T$ the scaled output vector, $\mathbf{U}_{\max} = \operatorname{diag}\left(\begin{bmatrix} \delta_{1\max} & \delta_{2\max} & \delta_{3\max} \end{bmatrix}\right)$ and $\mathbf{Y}_{\max} = \operatorname{diag}\left(\begin{bmatrix} a_{y1\max} & a_{y2\max} \end{bmatrix}\right)$ the scaling matrices. Open-loop simulations indicate that the TST starts to roll over at the tractor front axle wheel steer angle of 0.04 radian, which causes the tractor and the semitrailer to produce the lateral acceleration of 0.5 g $(4.9\ \mathrm{m/s^2})$. Hence, the scaling matrices are selected as $\mathbf{U}_{\max} = \operatorname{diag}\left(\begin{bmatrix} 0.04 & 0.1 & 0.1 \end{bmatrix}\right)$ and $\mathbf{Y}_{\max} = \operatorname{diag}\left(\begin{bmatrix} 4.9 & 4.9 \end{bmatrix}\right)$.

Since the RA ratio of the TST without ASS is greater than 1.0 within low to the crossover frequency range (see Figure 4), the objective of the MS controller design is to suppress the lateral acceleration of the semitrailer and force the RA ratio to approach 1.0. This is a disturbance attenuation problem and may be solved using the single DOF control (Skogestad and Postlethwaite, 2001; Gu et al., 2013) as shown in Figure 8. The exogenous disturbance δ_1 is weighted by the frequency function W_d, the output $\begin{bmatrix} a_{y1} & a_{y2} \end{bmatrix}^T$ by $\mathbf{W}_p$, the control input $\begin{bmatrix} \delta_2 & \delta_3 \end{bmatrix}^T$ by $\mathbf{W}_u$, and the measurement noise $\mathbf{n}$ by $\mathbf{W}_n$. A multi-input and multi-output MS controller $\mathbf{K}$ intends to minimise the weighted control input $\mathbf{e}_u$ and output $\mathbf{e}_{\ddot{y}}$. The RA characteristics of the TST with ASS can be manipulated by appropriate selection of the design parameters of the frequency weighting functions (Skogestad and Postlethwaite, 2001).

Figure 8 Single DOF control structure with frequency weighting functions

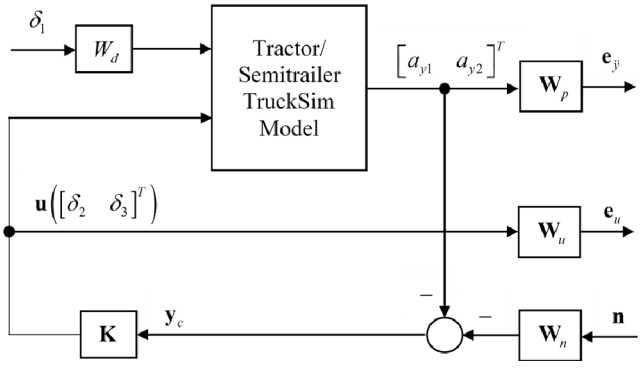

The frequency weighting functions are selected following the fundamental principles (Gu et al., 2013):

- an integral-shape high-gain low-pass filter weights the controlled output for accurate reference tracking
- a high-pass filter limits the control inputs at high frequencies and closed-loop bandwidth.

Thus, the weighting functions for the MS controller of the TST are selected as

$$W_d = k_{wd} \tag{14.1}$$

$$\mathbf{W}_n = \mathrm{diag}\left(\left[\begin{array}{cc} k_{wn1}\dfrac{n_{wn1}s+1}{d_{wn1}s+1} & k_{wn2}\dfrac{n_{wn2}s+1}{d_{wn2}s+1}\end{array}\right]\right) \tag{14.2}$$

$$\mathbf{W}_p = \mathrm{diag}\left(\left[\begin{array}{cc} \dfrac{s/M_1+w_{b1}}{s+w_{b1}A_1} & \dfrac{s/M_2+w_{b2}}{s+w_{b2}A_2}\end{array}\right]\right) \tag{14.3}$$

$$\mathbf{W}_u = \mathrm{diag}\left(\left[\begin{array}{cc} k_{wu1}\dfrac{(1/N_1)s+1}{Q_1s+1} & k_{wu2}\dfrac{(1/N_2)s+1}{Q_2s+1}\end{array}\right]\right). \tag{14.4}$$

The structure of the MS controller is shown in Figure 9, integrated with the TST model developed in TruckSim.

Figure 9 Structure of the TruckSim model integrated with the MS controller

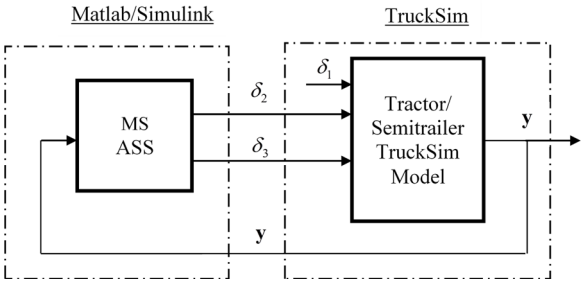

3.4 Design variable tuning using frequency-domain optimisation

The RA ratio in lateral acceleration is an important indicator of roll-over for the semitrailer. The RA frequency function of the TST provides complete information in a frequency range of interest. For an optimal trade-off between the manoeuvrability and the stability at high speeds, the RA frequency function should be restricted in the vicinity of 1.0. The design criterion is chosen as

$$\min_{0\le f\le f_u} \mathrm{obj} = \mathrm{RMS}\left\{RA(f)-1\right\} \text{ with respect to } \mathbf{X}_{\mathrm{ASS}}, \tag{15}$$

where $\mathbf{X}_{\mathrm{ASS}}$ is the design variable vector of the ASS controller to be optimised. For the SMC and NSMC based controllers, the $\mathbf{X}_{\mathrm{ASS}}$ involves the closed-loop poles and SMC gains; for the MS controller, the $\mathbf{X}_{\mathrm{ASS}}$ involves parameters of the frequency weighting

functions. The frequency upper bound f_u is chosen as the crossover frequency with trail-and-error method. The TST is excited with the MCSSI in a continuous mode, the RA frequency function $RA(f)$ is acquired using the AFRM technique, and the fitness value is calculated as the root-mean-square (RMS) of $RA(f)-1$ using equation (15). A genetic algorithm (GA) is utilised to search the optimal design variable vector to minimise the fitness value.

4 Results and discussion

The performance of the ASS controllers is evaluated using the simulations in the time-domain achieved under the low lateral acceleration SCSLA manoeuvre as shown Figure 2, and under a high lateral acceleration double lane change (DLC) manoeuvre. The ASS controllers are also examined with simulations performed under the continuous MCSSI manoeuvre using the AFRM technique.

4.1 Simulation results under the low lateral acceleration SCSLA manoeuvre

Figure 10 shows the time histories of lateral accelerations of the TST with the ASS controllers based on the LQR, SMC, NSMC, and the MS techniques under the simulated SCSLA manoeuvre. Compared with the result of the TST without ASS shown in Figure 3, the ASS controllers reduce the lateral accelerations of the tractor and the semitrailer, especially that of the semitrailer. The RA ratios for all ASS controllers approach 1.0 under the simulated SCSLA manoeuvre. Almost an identical RA ratio has been achieved by all the ASS controllers, and it is difficult to differentiate them under the low lateral acceleration manoeuvre.

Figure 11 shows the time histories of the active steering angles of the tractor rear axle wheel and the trailer axle wheel of the TST demanded by different ASS controllers under the SCSLA manoeuvre. The performance measure representing the energy consumed by the ASS actuators on the tractor rear axle and on that of the trailer axles can be calculated as $\frac{1}{2}\sum_{k=1}^{\infty}\delta_2^2(k)$ and $\frac{1}{2}\sum_{k=1}^{\infty}\delta_3^2(k)$ (k is the sampling index), respectively. Figure 12 illustrates the energy consumption measure corresponding to the ASS controller of LQR, SMC, NSMC, and MS under the SCSLA manoeuvre. It is indicated that in terms of energy consumption, the SMC controller is the most efficient, followed by the NSMC, LQR and MS, accordingly.

The main feature of the MS controller different from other ASS controllers is the phase-shift which makes the control command asynchronous with the system output measurements. This raises an issue regarding applying the AFRM technique. When measuring frequency responses using the AFRM technique, the vehicle is excited by the continuous MCSSI. Without phase-shift, the control effort induced over one sine wave cycle does not affect other cycles of the system. Thus, the input signal may have a zero initial value starting a new cycle, which makes the AFRM technique possible. The phase-shift makes the AFRM technique inapplicable. The phase-shift may be caused by frequency weighting without considering phase responses.

Figure 10 Time-histories of the lateral accelerations under the SCSLA manoeuvre for the TST with different ASS controllers: (a) LQR; (b) SMC; (c) NSMC and (d) MS

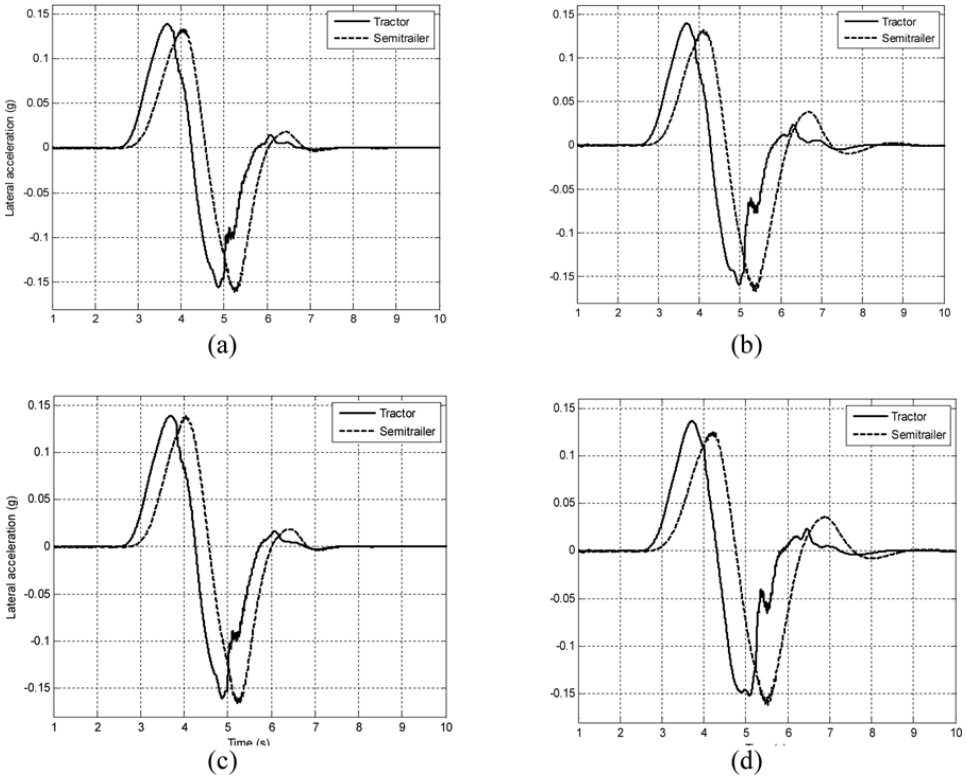

4.2 Simulation results based on frequency responses

Frequency responses of the TST with the ASS controllers of LQR, SMC, and NSMC are acquired using the AFRM technique. The amplitude of the MCSSI input is restricted to avoid exciting the nonlinear dynamics of the TST. Figure 13 shows the RA frequency responses in lateral acceleration of the TST without and with the ASS controllers of LQR, SMC, and NSMC. The ASS controllers of LQR, SMC and NSMC greatly improve the directional performance of the TST by means of keeping the RA ratio approximately near 1.0 within the frequency range of 0~0.6 Hz. Within the high frequency range of 0.6~1.0 Hz, the ASS controllers of SMC and NSMC outperform the LQR controller. For the TST without ASS, within the low frequency range, the RA is higher than that of the vehicle with ASS, but within the high frequency the RA is lower than that of the vehicle with ASS. Figure 13 shows that among the four cases, the SMC controller exhibits the highest robustness over the frequency range of 0~1.0 Hz.

4.3 Simulation results under the high lateral acceleration manoeuvre

The robustness of the directional performance of the TST with and without ASS at high lateral accerations is examined under the simulated DLC meanouver, under which the CG of the tractor follows the specified trajectory shown in Figure 14 at a constant forward

speed of 88 km/h. Three parameter uncertainty case studies, i.e., the trailer sprung mass, and the longitudinal and vertical positions of the trailer CG, are performed. To assess the robustness of the ASS controllers, a robustness index is originally defined. For a total of n (a positive integer) uncertain events in a given case study, the maximum (max), mean (mn), and minimum (min) values of the responses at a specific time instant may be obtained. By connecting all max-, mn-, and min-points, respectively, three curves can be obtained, representing the upper-bound, mean, and lower-bound of the responses of the n uncertain events. The robustness index is defined as the reciprocal of the area enclosed by the upper- and lower-bound curves for a specific performance measure. If the performance measure is the lateral acceleration of a vehicle unit, the robustness index has a unit of s/m. The robustness index in the lateral acceleration of the tractor with the LQR controller is defined as

$$R_{a_{y1\_lqr}} = \frac{1}{\int_0^{\infty} \left| a_{y1\_lqr\_\max}(t) - a_{y1\_lqr\_\min}(t) \right| \mathrm{d}t}, \tag{16}$$

where $a_{y1\_lqr\_\max}$ and $a_{y1\_lqr\_\min}$ denote the upper- and lower-bound of the tractor lateral acceleration responses in a case study with the LQR controller. All other robustness indices of the TST with other ASS controllers can be defined similarly.

Figure 11 Time histories of the active steering angle of the tractor rear axle wheels and trailer axle wheels under the SCSLA manoeuvre for the TST demanded by the ASS controller of: (a) LQR; (b) SMC; (c) NSMC and (d) MS

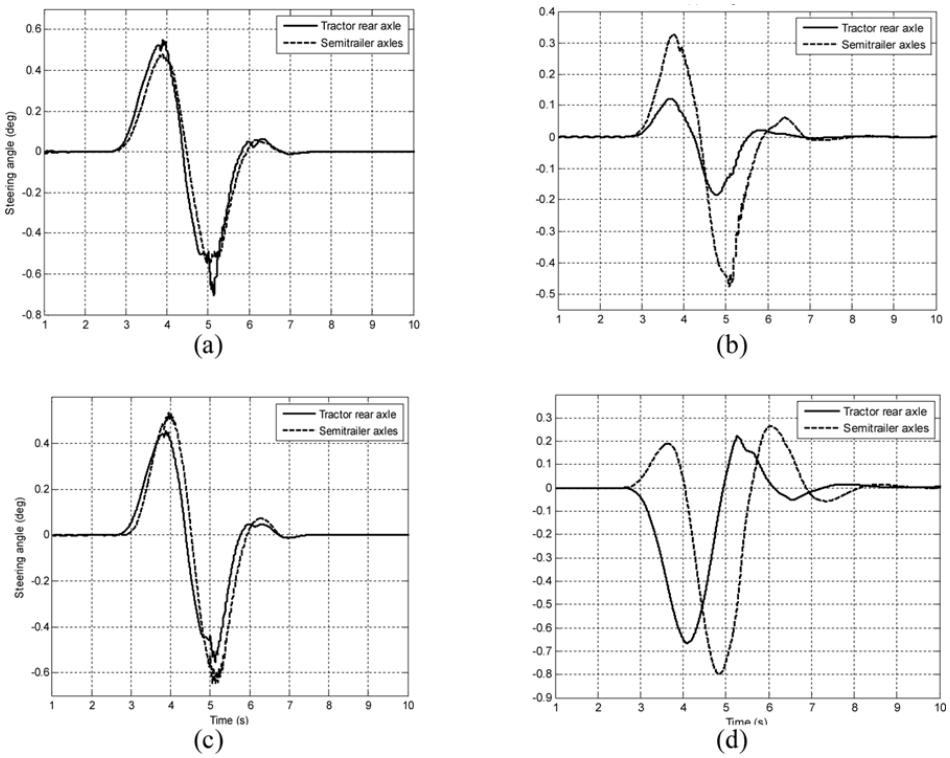

Figure 12 Energy consumption measure under the SCSLA manoeuvre for the TST with the ASS controller of LQR, SMC, NSMC, and MS (see online version for colours)

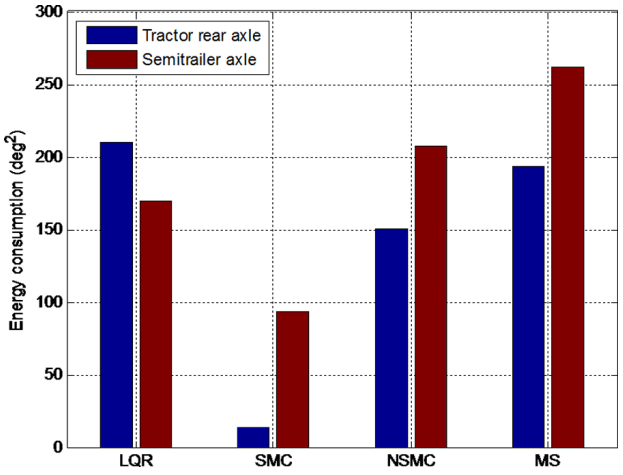

Figure 13 RA frequency response in lateral acceleration for the TST without and with ASS controllers of LQR, SMC and NSMC (see online version for colours)

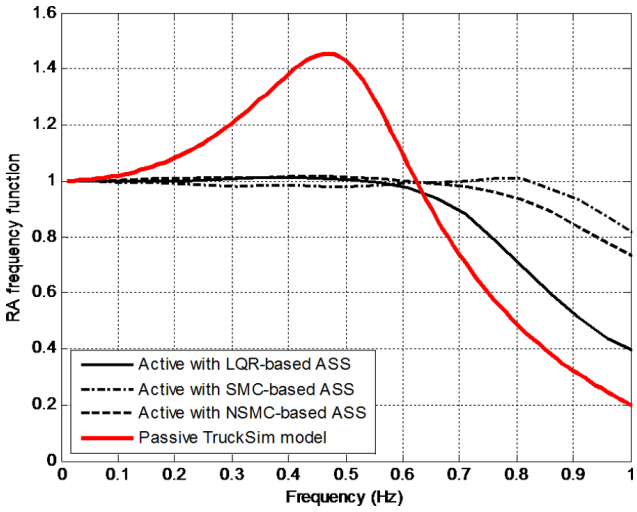

4.3.1 Case study on the uncertainty of semitrailer sprung mass

With the trailer sprung mass (including payload) varied from 0.5 to 2 times of the nominal value, i.e., $0.5m_{2\text{nom}} \le m_2 \le 2m_{2\text{nom}}$, the upper-, mean- and lower-bound responses in the lateral accelerations and active steering angles of the TST with LQR controller can be achieved, and the resulting responses are shown in Figure 15. It is shown that the LQR controller does not exhibit good robustness to the semitrailer sprung mass variation.

Figure 14 Target trajectory to be followed by the CG of the tractor under the DLC manoeuvre

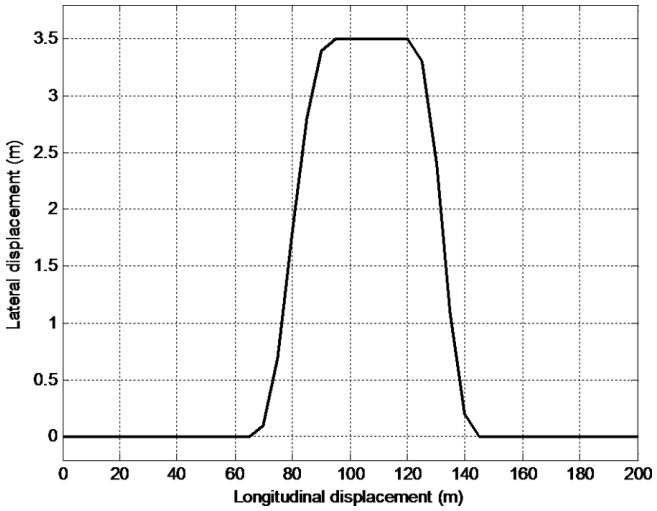

Figure 15 Responses of the TST with the LQR controller subject to the trailer sprung mass uncertainty: (a) tractor lateral acceleration; (b) semitrailer lateral acceleration; (c) tractor rear axle wheel steering angle and (d) semitrailer axle wheel steering angle (see online version for colours)

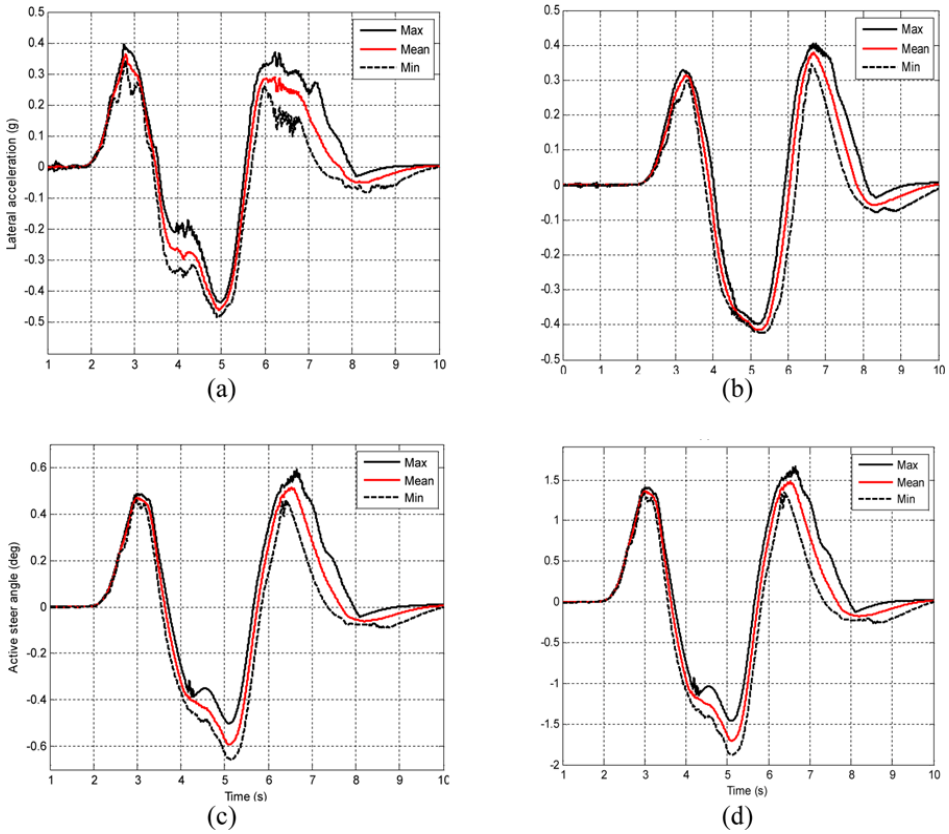

Figures 16–18 show the upper-, mean- and lower-bound curves of the lateral accelerations and active steering angles of the TST with the controllers of SMC, NSMC and MS, respectively. The corresponding robustness indices are listed in Table 1, and ploted in Figure 19. Among all the ASS controllers considered, the responses of the NSMC exhibit the most noisy curves, while the responses of the MS show the smoothest curves. The SMC controller is the most robust in tractor lateral acceleration, followed by the controllers of MS, NSMC and LQR; the controllers of SMC, MS and NSMC improve the robustness in tractor lateral acceleration by 93.22%, 77.3%, and 67.72%, respectively, with respect to the respective reference index value of the LQR controller. Similarly, the MS controller is the most robust in the semitrailer lateral acceleration, followed by the controllers of SMC, NSMC, and LQR; the controllers of MS, SMC, and NSMC improve the robustness in trailer lateral acceleration by 122.51%, 118.91%, and 7.01%, respectively, compared with the corresponding reference index value of the LQR controller. The MS controller is the most robust in tractor rear axle wheel steer angle, followed by the controllers of SMC, NSMC, and LQR. In terms of trailer axle wheel steer angle, the MS is the most robust, followed by the controllers of LQR, SMC, NSMC.

Figure 16 Responses of the TST with the SMC controller subject to the semitrailer sprung mass uncertainty: (a) tractor lateral acceleration; (b) semitrailer lateral acceleration; (c) tractor rear axle wheel steering angle and (d) semitrailer axle wheel steering angle (see online version for colours)

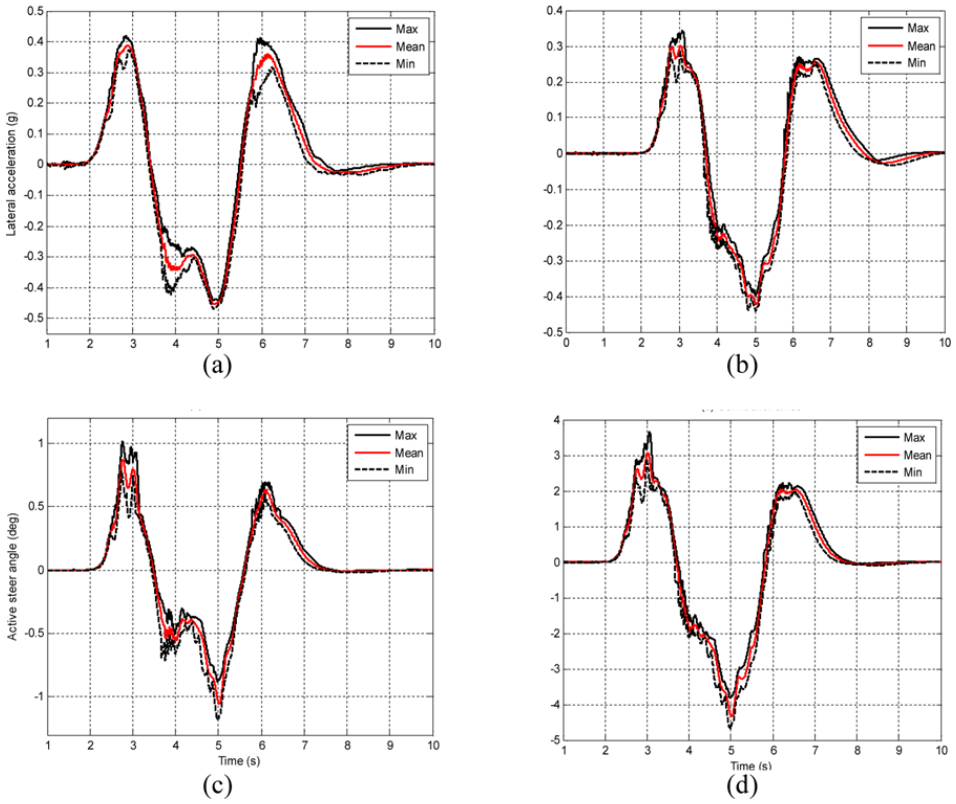

Figure 17 Responses of the TST with the NSMC controller subject to the semitrailer sprung mass uncertainty: (a) tractor lateral acceleration; (b) semitrailer lateral acceleration; (c) tractor rear axle wheel steering angle and (d) semitrailer axle wheel steering angle (see online version for colours)

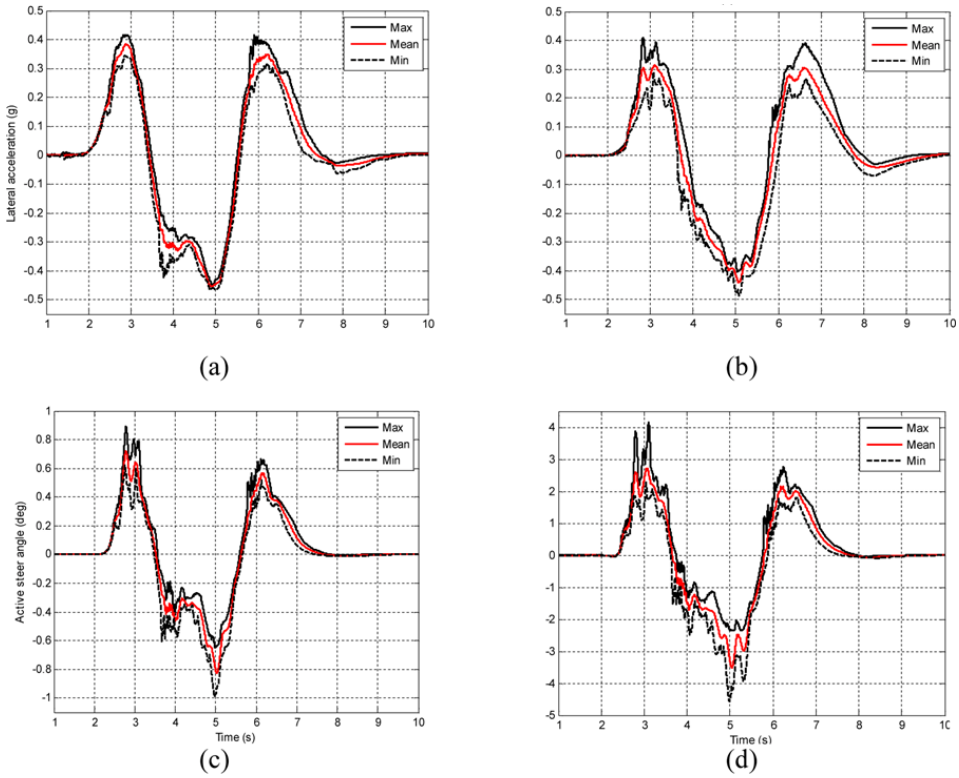

Table 1 Robustness indices of the TSTs with the ASS controllers subject to semitrailer sprung mass uncertainty

	LQR	*SMC*		*NSMC*		*MS*	
	$^{*}R_{idx}$	R_{idx}	$^{\#}R_{imp}$ (%)	R_{idx}	R_{imp} (%)	R_{idx}	R_{imp} (%)
$R_{a_{y1}}$ (s/m)	1.2728	2.4593	93.22	2.1348	67.72	2.2569	77.32
$R_{a_{y2}}$ (s/m)	1.4045	3.0746	118.91	1.5030	7.01	3.1252	122.51
$R_{\delta_2}\left(\frac{1}{\text{deg}\cdot\text{s}}\right)$	1.0380	1.2149	17.04	1.1716	12.87	1.5322	47.61
$R_{\delta_3}\left(\frac{1}{\text{deg}\cdot\text{s}}\right)$	0.3733	0.3567	–4.45	0.2154	-42.30	0.8113	117.33

$^{*}R_{idx}$ is the robustness index defined in equation (16).

$^{\#}R_{imp}$ is the relative improvement of the robustness with respect to that of the LQR controller.

Figure 18 Responses of the TST with the MS controller subject to the semitrailer sprung mass uncertainty: (a) tractor lateral acceleration; (b) semitrailer lateral acceleration; (c) tractor rear axle wheel steering angle and (d) semitrailer axle wheel steering angle (see online version for colours)

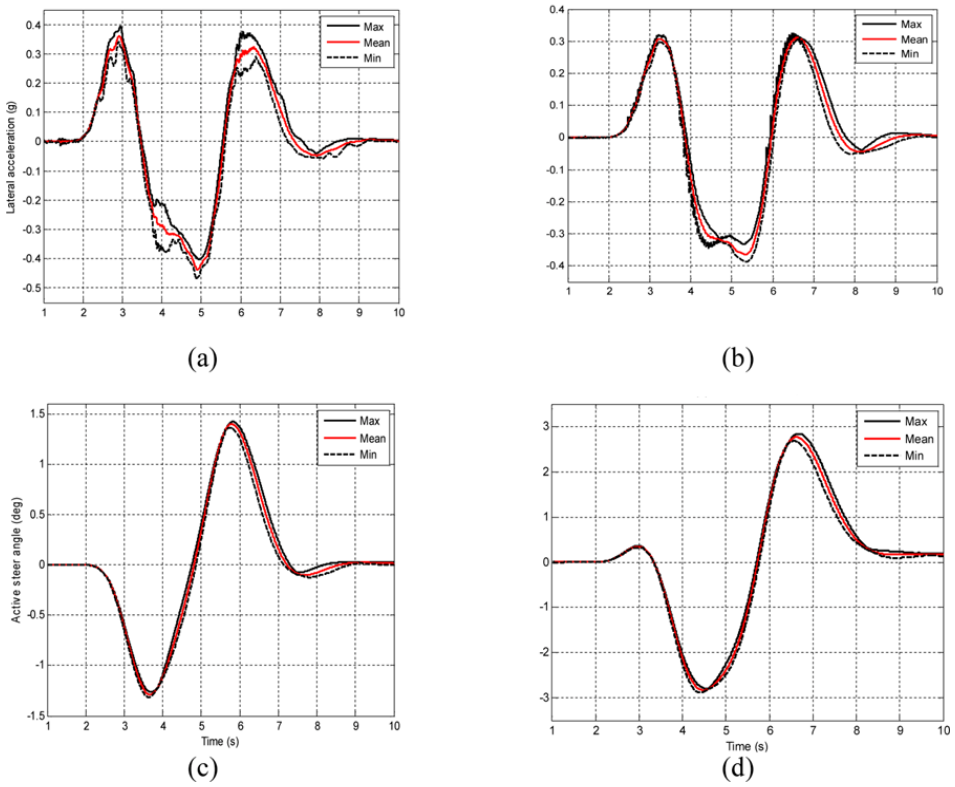

Figure 19 Robustness indices of the TST with different ASS controllers subject to the semitrailer sprung mass uncertainty: $R_{a_{y1}}(s/m)$ and $R_{a_{y2}}(s/m)$, $R_{\delta_2}\ (1/\text{deg}\cdot s)$ and $R_{\delta_2}\ (1/\text{deg}\cdot s)$ (see online version for colours)

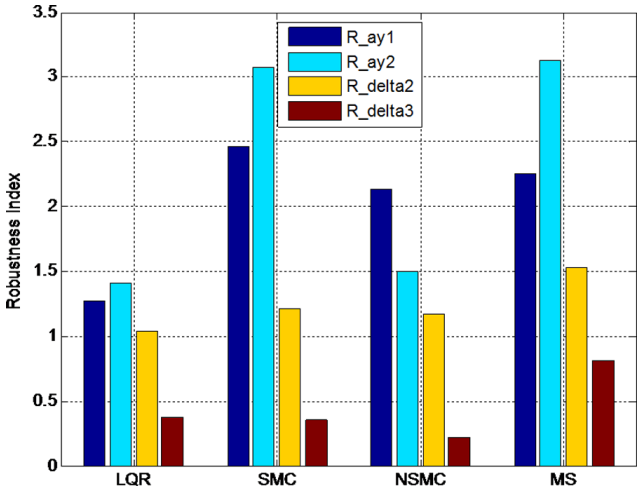

4.3.2 Case study on the uncertainty of trailer CG longitudinal position

The robustness of the directional performance of the TST with different ASS controllers is examined under the simulated DLC manoeuvre subjet to the variation of trailer CG longitudinal position in the range of 0.4 to 1.25 times of the nominal value $\left(0.4l_{21\text{nom}} \le l_{21} \le 1.25l_{21\text{nom}}\right)$. The robustness indices of lateral acceleration and steer angles of tractor rear wheels and trailer wheels for the controllers of LQR, SMC, NSMC, and MS are listed in Table 2 and shown in Figure 20.

Table 2 Robustness indices of the TST with different ASS controllers subject to the variation of trailer CG longitudinal position

	LQR	*SMC*		*NSMC*		*MS*	
	$^{*}R_{idx}$	R_{idx}	$^{\#}R_{imp}$ (%)	R_{idx}	R_{imp} (%)	R_{idx}	R_{imp} (%)
$R_{a_{y1}}$ (s/m)	0.9574	1.4512	51.58	1.5202	58.78	1.5331	60.13
$R_{a_{y2}}$ (s/m)	1.2444	1.3307	6.93	1.1509	–7.51	1.5214	22.26
$R_{\delta_2}\left(\frac{1}{\text{deg·s}}\right)$	0.5134	0.6330	23.29	0.5752	12.04	0.9036	76.00
$R_{\delta_3}\left(\frac{1}{\text{deg·s}}\right)$	0.1824	0.2507	37.44	0.1364	–25.22	0.2374	30.15

$^{*}R_{idx}$ is the robustness index defined in equation (16).

$^{\#}R_{imp}$ is the relative improvement of the robustness with respect to that of the LQR controller.

Compared with the indices shown in Figure 19, those seen in Figure 20 are lower. This implies that the ASS controllers be more sensitive to the variation of the trailer CG longitudinal position than to the change of trailer sprung mass. Furthermore, subject to the variation of trailer CG longitudinal position, the simulation results confirm that the MS controller is the most robust, whereas the LQR controller is the least robust; in between, the controllers of SMC and NSMC exhibit comparable robustness. The controllers of SMC, NSMC and MS improve the robustness in tractor lateral acceleration by 51.58%, 58.78%, and 60.13%, and in trailer lateral acceleration by 6.93%, –7.51% and 22.26%, respectively, with respect to the corresponding indices of the LQR controller.

4.3.3 Case study on the uncertainty of trailer CG vertical position

The robustness of the ASS controllers is evaluated under the simulated DLC manoeuvre subject to the variation of trailer CG vertical position in the range of 1–2 times of the nominal value, i.e., $h_{CGnom} \le h_{CG} \le 2h_{CGnom}$. The resulting robustness indices are listed in Table 3 and plotted in Figures 21 and 22. Compared with the aforementioned parameter uncertainties considered, the ASS controllers are more robust to the uncertainty of trailer CG vertical position.

Figure 20 Robustness indices of the TST with different ASS controllers subject to the variation of trailer CG longitudinal position: $R_{a_{y1}}(s/m)$ and $R_{a_{y2}}(s/m)$, R_{δ_2} $(1/\deg\cdot s)$ and R_{δ_2} $(1/\deg\cdot s)$ (see online version for colours)

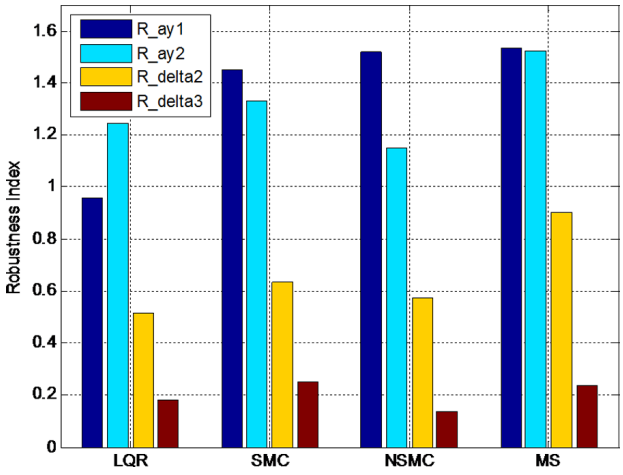

Table 3 Robustness indices of the TST with different ASS controllers subject to the variation of trailer CG vertical position

	LQR	SMC		NSMC		MS	
	$^{*}R_{idx}$	R_{idx}	$^{\#}R_{imp}$	R_{idx}	R_{imp}	R_{idx}	R_{imp} (%)
$R_{a_{y1}}$ (s/m)	4.8055	3.3703	–29.86%	3.8163	–20.58%	5.8206	21.12
$R_{a_{y2}}$ (s/m)	5.3614	1.9484	–63.66%	2.4276	–54.72%	4.1696	–22.23
$R_{\delta_2}\left(\frac{1}{\deg\cdot s}\right)$	3.0907	811.8262	261.67	652.8228	210.22	4.3049	39.29
$R_{\delta_3}\left(\frac{1}{\deg\cdot s}\right)$	1.1038	299.7797	270.59	111.4278	99.95	1.6108	45.93

$^{*}R_{idx}$ is the robustness index defined in equation (16).

$^{\#}R_{imp}$ is the relative improvement of the robustness with respect to that of the LQR controller.

The results disclose a phenomenon that the LQR and MS controllers outperform the SMC and NSMC controllers. In terms of the steer angles of tractor rear wheels and trailer wheels, the SMC and NSMC controllers are not sensitive to the variation of trailer CG vertical position. This observation may be interpreted by the fact that the trailer CG vertical position mainly affect the inertia properties of the roll dynamics of the trailer; and the coupling of the roll dynamics and yaw dynamics of the TST is loose. The SMC and NSMC controllers work on the full states of the yaw-plane models which are least affected by the roll dynamics related parameter uncertainty. However, the LQR and MS controllers are designed considering the vehicle units' lateral accelerations, which are dependent on the roll dynamics of the TST. The MS controller has the robustness index increased by 21.12% in tractor acceleration, decreased 22.23% in trailer lateral acceleration, increased 39.29% in tractor rear axle wheel steer angle, and increased

45.29% in trailer wheel steer angle, with respect to the corresponding robustness indices of the LQR controller.

Figure 21 Robustness indices (s/m) in vehicle unit lateral acceleration of the TST with different ASS controllers subject to the variation of trailer CG vertical position (see online version for colours)

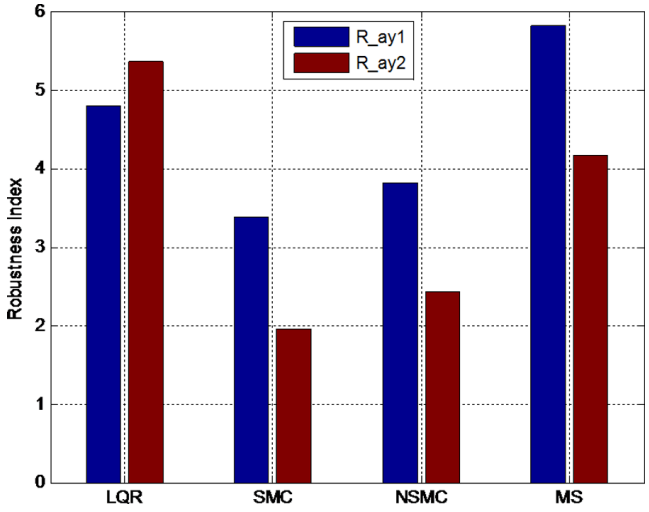

Figure 22 Robustness indices $(1/\deg \cdot s)$ in steer angle of tractor rear wheels and trailer wheels of the TST with different ASS controllers subject to the variation of trailer CG vertical position (see online version for colours)

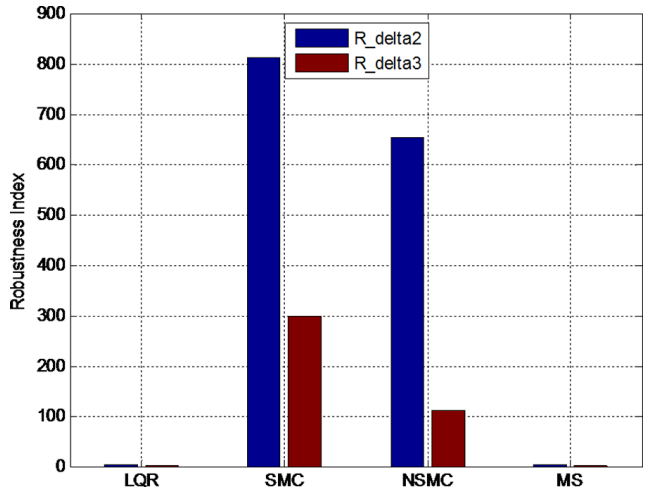

5 Conclusions

Three robust ASS controllers, namely, the SMC, NSMC and MS, have been studied for improving the manoeuvrability and the stability of AHVs at high speeds. To evaluate the

robustness of the ASS controllers, co-simulations are conducted by integrating the ASS controllers designed in Matlab/Simulink software and a nonlinear TST model developed in TruckSim package. The MS-based controller differs from the others by introducing phase-shift into the control command, which makes the AFRM technique inapplicable. With the AFRM technique, the design variables of the controllers based on the LQR, SMC, and NSMC techniques are optimised by using a genetic algorithm for the optimal trade-off between the manoeuvrability and stability in a frequency range of interest. A robustness index has been proposed to quantify the robust performance of the ASS controllers based on the LQR, SMC, NSMC and MS techniques under high lateral acceleration manoeuvres.

The simulation results show that it is hard to differentiate the ASS controllers under low lateral acceleration manoeuvres. Under high lateral acceleration manoeuvres, the ASS controllers demonstrate different robustness to parametric uncertainties. Among the uncertainties considered, the ASS controllers are the most robust to the uncertainty of the vertical trailer CG position and the least robust to the variation of the longitudinal trailer CG position. Among all the ASS controllers investigated, the MS is the most robust to the uncertainties of the trailer mass and the longitudinal trailer CG position. Subject to the uncertainty of vertical trailer sprung mass CG position, the robustness of the LQR and MS based controllers is comparable, and these controllers outperform the SMC and NSMC based controllers.

Acknowledgements

Financial support of this research by the Natural Science and Engineering Research Council of Canada (Grant No. RGPIN/327063-2012) is gratefully acknowledged.

References

Aurell, J. and Winkler, C.B. (1995) 'Standard test procedures for the lateral stability of heavy vehicle combinations', *Road Transport Technology*, Vol. 4, University of Michigan Transportation Research Institution, Ann Arbor, pp.463–471.

Busch, J. and Bestle, D. (2014) 'Optimisation of lateral car dynamics taking into account parameter uncertainties', *Vehicle System Dynamics: International Journal of Vehicle Mechanics and Mobility*, Vol. 52, No. 2, pp.166–185.

Cheng, C., Roebuck, R., Odhams, A. and Cebon, D. (2011) 'High-speed optimal steering of a tractor-semitrailer', *Vehicle Systems Dynamics*, Vol. 49, No. 4, pp.561–593.

Cheng, J.F. and Cebon, D. (2008) 'Improving roll stability of articulated vehicles using active semi-trailer steering', *Vehicle Systems Dynamics*, Vol. 46, Supplement, pp.373–388.

Ding, X., He, Y., Ren, J. and Sun, T. (2012) 'A comparative study of control algorithms for active trailer steering systems of articulated heavy vehicles', *American Control Conference*, Montreal, Manuscript ID: (1090).

Ding, X., Mikaric, S. and He, Y. (2013) 'Design of an active trailer-steering system for multi-trailer articulated heavy vehicles using real-time simulations', *Proceedings of the Institution of Mechanical Engineers, Part D: Journal of Automobile Engineering*, Vol. 227, pp.643–655.

Doumiati, M., Sename, O., Dugard, L., Martinez, J., Gaspar, P. and Szabo, Z. (2013) 'Integrated vehicle dynamics control via coordination of active front steering and rear braking', *European Journal of Control*, Vol. 19, No. 2, pp.121–143.

Doyle, J.C. (1985) 'Structured uncertainty in control system design', *Proceedings of the 24 IEEE Conference on Decision and Control*, Fort Lauderdale, Florida, USA, pp.260–265.

Doyle, J.C. (1987) 'A review of μ: for case studies in robust control', *Proceedings of 10th IFAC World Congress*, Munich, Germany, pp.395–402.

Ervin, R. and MacAdam, C. (1982) *The Dynamic Response of Multiply-Articulated Truck Combinations to Steering Input*, SAE Technical Paper 820973.

Fernandes, A.A. and Alcalde, V.H.C. (2007) 'Serious compensation using variable structure and lyapunov function controls for stabilization multimachine power system', *Mediterranean Conference on Control and Automation*, Med., pp.1–6.

Gao, X., Mcvey, B.D. and Tokar, R.L. (1995) 'Robust controller design of four wheel steering systems using μ synthesis technique', *Proceedings of the 34th Conference on Decision and Control*, New Orleans, LA, pp.875–882.

Gu, D.W., Petkov, P.H. and Konstantinov, M.M. (2013) *Robust Control Design with Matlab*, 2nd ed., Springer-verlag London.

Habibi, S.R. and Richards, R.J. (1992) 'Sliding mode control of an electrically powered industrial robot', *IEE Proceedings D: Control Theory and Applications*, Vol. 139, No. 2, pp.207–225.

He, Y. and Islam, M.M. (2012) 'An automated design method for active trailer steering systems of articulated heavy vehicles', *ASME Journal of Mechanical Design*, Vol. 134, pp.041002.

He, Y., Islam, M.M. and Webster, T. (2010) 'An integrated design method for articulated heavy vehicles with active trailer steering systems', *SAE International Journal of Passenger Cars-Mechanical Systems*, Vol. 119, No. 6, pp.158–174.

Huang, H.H., Yedavalli, R.K. and Guenther, D.A. (2012) 'Active roll control for rollover prevention of heavy articulated vehicles with multiple-rollover –index minimization', *Vehicle Systems Dynamics*, Vol. 50, No. 3, pp.471–493.

Islam, M.M., Ding, X. and He, Y. (2012) 'A closed-loop dynamic simulation based design method for articulated heavy vehicles with active trailer steering systems', *Vehicle Systems Dynamics*, Vol. 50, No. 5, pp.675–697.

Islam, M.M., He, Y., Zhu, S. and Wang, Q. (2014) 'A comparative study of multi-trailer articulated heavy vehicle models', *Proceedings of the Institution of Mechanical Engineers, Part D: Journal of Automobile Engineering*, Vol. 229, No. 9, pp.1200–1228.

Kharrazi, S. (2012) *Steering Based Lateral Performance Control of Long Heavy Vehicle Combinations*, Thesis for the Degree of Doctor of Philosophy, Chalmers University of Technology, Gothenburg, Sweden.

Kulebakin, V. (1932) *On Theory of Vibration Controller for Electric Machines* (in Russian).

Lin, F.J., Lin, C.H. and Shen, P.H. (2002) 'Variable structure control for linear synchronous motor using recurrent fuzzy neural network', *IECON Proceedings* (*Industrial Electronics Conference*), Vol. 3, pp.2108–2113.

Maciejowski, J.M. (1989) *Multivariable Feedback Design*, Addison Wesley, Workingham, England.

Mao, X. and Lu, K. (2008) 'Research on the nonlinear governor of diesel engine with variable structure control theory', *IEEE International Conference on Robotics, Automation and Mechanics*, Chengdu, China, pp.537–542.

Miege, A.J.P. and Cebon, D. (2005) 'Optimal roll control of an articulated vehicle: theory and model validation', *Vehicle Systems Dynamics*, Vol. 43, No. 12, pp.867–893.

MSC (2014) 'Mechanical simulation corporation', *TruckSim Options*, https://www.carsim.com/products/trucksim/packages.php

Nikolski, G. (1934) 'On automatic stability of a ship on a given course', *Proceedings of the Central Communication Laboratory*, Vol. 1, pp.34–75.

Nise, N.S. (2011) *Control Systems Engineering*, 6th ed., John Wiley & Sons, Inc., Hoboken, UK.

Oreh, S.H.T., Kazemi, R. and Azadi, S. (2014) 'A sliding-mode controller for directional control of articulated heavy vehicles', *Proceedings of the Institute of Mechanical Engineers Part D: Journal of Automobile Engineering*, Vol. 228, No. 3, pp.245–262.

Pacejka, H. (2005) *Tyre and Vehicle Dynamics*, Butterworth-Heinemann, Oxford.

Palkovics, L. and El-Gindy, M. (1996) 'Examination of different control strategies of heavy-vehicle performance', *Journal of Dynamic Systems, Measurement* and *Control*, Vol. 118, pp.489–498.

Palkovics, L., Ilosvai, L. and Semsey, A. (1994) 'The self-steering behaviour of a tractor-semitrailer at high-speed and its control to improve lateral stability', *Heavy Vehicle Systems, International Journal of Vehicle Design*, Vol. 1, No. 3, pp.304–323.

Rangavajhula, K. and Tsao, H.S.J. (2008) 'Command steering of trailers and command-steering-based optimal control of an articulated system for tractor-track following', *Proceedings of Institute of Mechanical Engineers, Part D: Journal of Automobile Engineering*, Vol. 222, pp.935–954.

SAE (1993) *A Test for Evaluating the Rearward Amplification of Multi-Articulated Vehicles*, SAE Recommended Practice J2179, Society of Automotive Engineers, Warrendale, USA.

Skogestad, S. and Postlethwaite, I. (2001) *Multivariable Feedback Control Analysis and Design*, 2nd ed., John Wiley & Sons, New York, USA.

Slotine, J.E. and Li, W. (1991) *Applied Nonlinear Control*, Prentice-Hall, New Jersey.

Utkin, V. (1977) 'Variable structure systems with sliding mode', *IEEE Transactions on Automatic Control*, Vol. 22, No. 2, pp.212–222.

Utkin, V., Guldner, J. and Shi, J. (1999) *Sliding Mode Control in Electromechanical Systems*, Taylor and Francis, Philadelphia, USA.

Wang, J.Y. and Tomizuka, M. (2000) 'Dynamic analysis and robust steering controller design for automated lane guidance of heavy-duty vehicles', *Asian Journal of Control*, Vol. 2, No. 3, pp.140–154.

Yin, G.D., Chen, N., Wang, J.X. and Chen, J.S. (2010) 'Robust control for 4WS vehicles considering a varying tire-road friction coefficient', *International Journal of Automotive Technology*, Vol. 11, No. 1, pp.33–40.

Zhu, S. and He, Y. (2015) 'Articulated heavy vehicle lateral dynamic analysis using an automated frequency response measuring technique', *International Journal of Vehicle Performance*, Vol. 2, No. 1, pp.30–57.

Zhu, S., Ni, Z. and He, Y. (2017) 'An investigation of test manoeuvres for determining rearward amplification of articulated heavy vehicles', Submitted to *Vehicle System Dynamics*, Manuscript ID: NVSD-2017-0049.

Appendix 1: System matrices

The system matrices for the linear model in equation (1) are given as

$$\mathbf{M} = \begin{bmatrix} -(l_{c1}+l_{c21})m_2 & -l_{c21}m_2 & (m_1+m_2)U_1 & 0 \\ I_{zz1}+l_{c1}(l_{c1}+l_{c21})m_2 & l_{c1}l_{c21}m_2 & -l_{c1}m_2U_1 & 0 \\ I_{zz2}+l_{c21}(l_{c1}+l_{c21})m_2 & I_{zz2}+l_{c21}^2m_2 & -l_{c21}m_2U_1 & 0 \\ 0 & 0 & 0 & 1 \end{bmatrix}.$$

$\mathbf{P} \in \mathbf{R}^{4\times 4}$. The non-zero elements of matrix $\mathbf{P}$ are given as

$$P(1,1) = \frac{(l_{c21} + b_{23} + l_{c1})C_{r23} - C_{f11}a_{11} + C_{r12}b_{12}}{U_1} - (m_1 + m_2)U_1,$$

$$P(1,2) = \frac{(l_{c21} + b_{23})C_{r23}}{U_1},$$

$$P(1,3) = -(C_{f11} + C_{r12} + C_{r23}),\ P(1,4) = C_{r23},$$

$$P(2,1) = m_2 l_{c1} U_1 - \frac{(l_{c1} + b_{23} + l_{c21})C_{r23}l_{c1} + C_{f11}a_{11}^2 + C_{r12}b_{12}^2}{U_1},$$

$$P(2,2) = -\frac{(l_{c21} + b_{23})C_{r23}l_{c1}}{U_1},\ P(2,3) = C_{r12}b_{12} - C_{f11}a_{11} + C_{r23}l_{c1},\ P(2,4) = -C_{r23}l_{c1},$$

$$P(3,1) = m_2 l_{c21} U_1 - \frac{(l_{c21} + b_{23} + l_{c1})C_{r23}(l_{c21} + b_{23})}{U_1},\ P(3,2) = -\frac{(l_{c21} + b_{23})^2 C_{r23}}{U_1},$$

$$P(3,3) = (l_{c21} + b_{23})C_{r23},\ P(3,4) = -(l_{c21} + b_{23})C_{r23},\ P(4,2) = 1.$$

$$\mathbf{H}_1 = \begin{bmatrix} C_{f11} \\ C_{f11}a_{11} \\ 0 \\ 0 \end{bmatrix},\ \mathbf{H}_2 = \begin{bmatrix} C_{r12} \\ -C_{r12}b_{12} \\ 0 \\ 0 \end{bmatrix} \text{ and } \mathbf{H}_3 = \begin{bmatrix} C_{r23} \\ -C_{r23}l_{c1} \\ -C_{r23}(l_{c21} + b_{23}) \\ 0 \end{bmatrix}.$$

$$\mathbf{C} = \begin{bmatrix} U_1\mathbf{A}(3,:) + [U_1 \quad 0 \quad 0 \quad 0] \\ -(l_{c21} + l_{c1})\mathbf{A}(1,:) - l_{c21}\mathbf{A}(2,:) + U_1\mathbf{A}(3,:) + [U_1 \quad 0 \quad 0 \quad 0] \end{bmatrix},$$

$$\mathbf{D} = \begin{bmatrix} U_1\mathbf{B}_2(3,:) & U_1\mathbf{B}_3(3,:) \\ -(l_{c21} + l_{c1})\mathbf{B}_2(1,:) - l_{c21}\mathbf{B}_2(2,:) + U_1\mathbf{B}_2(3,:) & -(l_{c21} + l_{c1})\mathbf{B}_3(1,:) - l_{c21}\mathbf{B}_3(2,:) + U_1\mathbf{B}_3(3,:) \end{bmatrix},$$

$$\mathbf{D}_1 = \begin{bmatrix} U_1\mathbf{B}_1(3,:) \\ -(l_{c21} + l_{c1})\mathbf{B}_1(1,:) - l_{c21}\mathbf{B}_1(2,:) + U_1\mathbf{B}_1(3,:) \end{bmatrix}.$$

The system matrices for the nonlinear model in equation (2) are given as

$$\mathbf{P}_{nl} = \begin{bmatrix} 0 & 0 & 1 & 0 \\ 0 & -(m_1U_1 + m_2U_2) & 0 & 0 \\ 0 & l_{c1}m_2U_2 & 0 & 0 \\ 0 & l_{c21}m_2U_2 & 0 & 0 \end{bmatrix} \text{ and } \mathbf{H}_{nl} = \begin{bmatrix} a_{11} & -b_{12} & -l_{c1} \\ 0 & 0 & -b_{23} - l_{c21} \\ 0 & 0 & 0 \\ 1 & 1 & 1 \end{bmatrix},$$

$$\mathbf{C}_{nl} = \begin{bmatrix} U_1\mathbf{A}_{nl}(3,:) + [U_1 \quad 0 \quad 0 \quad 0] \\ -(l_{c21} + l_{c1})\mathbf{A}_{nl}(1,:) - l_{c21}\mathbf{A}_{nl}(2,:) + U_1\mathbf{A}_{nl}(3,:) + [U_1 \quad 0 \quad 0 \quad 0] \end{bmatrix},$$

$$\mathbf{D}_{nl} = \begin{bmatrix} U_1 \mathbf{B}_{nl}(3,:) \\ -(l_{c21} + l_{c1})\mathbf{B}_{nl}(1,:) - l_{c21}\mathbf{B}_{nl}(2,:) + U_1 \mathbf{B}_{nl}(3,:) \end{bmatrix}.$$

Appendix 2: Notation and nominal values of the parameters

Table A1 Notation and nominal values of the parameters

Parameters	*Description*	*Units*	*Nominal values*
a_{11}	Longitudinal distance between tractor front axle and tractor total mass CG	m	1.115
a_{y1}	Lateral acceleration of the tractor unit	m/s^2	
$\overline{a}_{y1}$	Scaled lateral acceleration of the tractor unit		
a_{y2}	Lateral acceleration of the semitrailer unit	m/s^2	
$\overline{a}_{y2}$	Scaled lateral acceleration of the semitrailer unit		
b_{12}	Longitudinal distance between tractor rear axle and tractor total mass CG	m	2.585
C_{f11}	Tyre corning stiffness of the tractor front axle	N/rad	422,636
C_{r12}	Tyre corning stiffness of the tractor rear axle	N/rad	1,033,500
C_{r23}	Tyre corning stiffness of the semitrailer axles	N/rad	1,108,968
b_{23}	Longitudinal distance between trailer total mass CG and trailer middle axle	m	2.047
F_1	Lateral tyre force of the tractor front axle	N	
F_2	Lateral tyre force of the tractor rear axle	N	
F_3	Lateral tyre force of the semitrailer axles	N	
I_{zz1}	Moment of inertia of tractor total mass	kg.m^2	12,386
I_{zz2}	Moment of inertia of trailer total mass	kg.m^2	225,317
l_{c1}	Longitudinal distance between tractor total mass CG and fifthwheel	m	1.959
l_{c21}	Longitudinal distance between trailer total mass CG and fifthwheel	m	5.653
m_1	Tractor total mass	kg	6,525
m_2	Trailer total mass	kg	33,221
U_1	Forward speed of the tractor unit	m/s	
U_2	Forward speed of the semitrailer unit	m/s	
β_1	Side-slip angle of the tractor unit	rad	

Table A1 Notation and nominal values of the parameters (continued)

Parameters	*Description*	*Units*	*Nominal values*
δ_1	Steering angle of tractor front axle	rad	
$\bar{\delta}_1$	Scaled steering angle of tractor front axle		
δ_2	Steering angle of the tractor rear axle	rad	
$\bar{\delta}_2$	Scaled steering angle of the tractor rear axle		
δ_3	Steering angle of the semitrailer axles	rad	
$\bar{\delta}_3$	Scaled steering angle of the semitrailer axles		
ψ_1	Yaw angle of tractor CG	rad	
$\Delta\psi$	Articulation angle between the tractor and semitrailer unit	rad	